Archives of Mechanics • Archiwum Mechaniki Stosowanej • 27, 1, pp. 157–172, Warszawa 1975

On dilatational effects of inelastic granular media(*)

T. HUECKEL and A. DRESCHER (WARSZAWA)

AN INCREMENTAL elastic-plastic model of granular material is proposed. The theory is based on dilatational plasticity for irreversible part of deformation and hypoelasticity for reversible part. The hardening and hypoelastic moduli are postulated to be functions of density changes. The resulting coupling of reversible and irreversible deformation laws is discussed. The experiments were carried out in the uniaxial strain state on several granular media (e.g. wheat and rice grains) and compared with theoretical solution. The procedure for determination of material functions is presented.

W pracy przedstawiono przyrostowy model sprężysto-plastycznego ośrodka rozdrobnionego. Koncepcję modelu oparto na dylatacyjnej teorii plastyczności formułując prawo nieodwracalnych przyrostów deformacji oraz na hiposprężystości dla przyrostów odwracalnych. Przyjęto, że moduł wzmocnienia oraz moduły hiposprężyste są funkcjami zmiany gęstości. Przedyskutowano wynikające z tego założenia sprzężenie deformacji odwracalnych i nieodwracalnych. W celu zweryfikowania teorii przeprowadzono badania doświadczalne w jednoosiowym stanie odkształcenia na kilku materiałach rozdrobnionych (pszenicy, ryżu, piasku), których wyniki porównano z wynikami rozwiązania teoretycznego. Pokazano ponadto algorytm wyznaczania funkcji materiałowych występujących w teorii.

В работе представлена модель в приростах упруго-пластической сыпучей среды. Концепция модели опирается на дилатационной теории пластичности, формулируя закон необратимых приростов деформации, а также на гипоупругости для обратимых приростов. Принято, что модуль упрочнения и гипоупругие модули являются функциями изменения плотности. Обсуждено, вытекающее из этого предположения, сопряжение обратимых и необратимых деформаций. С целью проверки теории проведены экспериментальные исследования в одноосном деформационном состоянии на нескольких сыпучих материалах (пшеница, рис, песок), результаты которых сравнены с результатами теоретического решения. Кроме этого дается алгоритм определения материальных функций выступающих в теории.

1. Introduction

IN RECENT years, there has been a considerable effort toward analytical description of mechanical behaviour of inviscid granular media in the range of irreversible deformation. Apart from the complexity of physical and chemical structure and variety of natural and artificial granular materials like soils, grain, sugar, cement, chemical powders there are some mechanical phenomena which are observed for majority of them [1, 2, 3]. The main feature of their mechanical behaviour is its loading or deformation path dependence. For a given loading-unloading programme it is clearly manifested by: i) different material response for loading and for unloading, what can be distinguished even for a very small cycle, and ii) the dependence of the both loading and unloading behaviour on stress or strain level reached in loading range. Therefore it seems to be natural to formulate the physical relations in increments, and to distinguish the additive reversible and irreversible parts of strain increment relating them to two mechanisms of deformations.

The above assumptions are well known in the theory of metal plasticity with the linear Hooke's law for reversible and the work or strain-hardening plasticity for irreversible

(*) The paper presented at the Conference on Applied Mechanics, June 12–15, 1972 in Sandomierz.

part of strain-increment. The application of these models is legitimate for metals by the crystal atomic net deformation and dislocation movement, what of course cannot be referred to granular media.

One of the main parameters affecting the behaviour of granular materials is their actual porosity. During the deformation process the grain arrangement varies resulting in macroscopically observed volume changes. Therefore it seems reasonable to relate the variation of mechanical properties to variation of material density. We shall not make any distinction between density variation due to compressibility of particles and void changes, thus accounting only for bulk density variation in a macroscopically uniform representative element. Starting from this concept, several dilatational theories of plasticity have been suggested, to begin with DRUCKER, GIBSON and HENKEL [4], JENIKE and SHIELD [5], ROSCOE with his group [6, 7] and developed in numerous publications [8–15]. However, in these papers the main interest is given to the mechanism of the irreversible deformations, while the mechanism of the reversible deformations is treated rather simply.

The aim of the present paper is to discuss the application to granular materials of an incremental theory of the reversible and irreversible deformations, which as far as possible follows the dilatational theory of plasticity, but which also incorporates the variation of unloading curves with irreversible deformation induced during the loading process.

Recently, several attempts were made to apply the incremental laws in description of mechanical response during loading and unloading programme. Such incremental relations werei nvestigated by HOLUBEC [1] for triaxial test on the initially orthotropic sand. COON and EVANS [16] discussed the incremental equations for reversible strains and their connection with elasticity relations. These authors suggested two different approaches (elastic and hypoelastic) to the description of mechanical behaviour reffering to Holubec data. A model of material with variable stiffness moduli during loading, unloading and reloading was proposed and tested by NELSON and BARON [17]. Very recently BALADI [19] has shown an application of a non-linear elastic-plastic model.

In our paper, following [18], it is postulated that both irreversible and reversible strain increments depend on the current density. The resulting consequences are discussed regarding specific form of dependence. In particular, if the material functions of the reversible strain increment depend on the irreversible change of the density, the coupling of the mechanisms generating reversible and irreversible deformations occurs. The coupling results in stiffening of the material in subsequent unloadings for consolidation or in softening for dilatation. The related phenomena are known for various porous materials as well as for fissured concrete and rocks.

To compare the behaviour of the model presented with that of real granular mass, the experiments were carried out on such natural materials as wheat grains, rice grains, sand, and on rubber balls.

The problem investigated here is of considerable practical interest, since in many cases both loading and unloading processes occur and should be accounted for in the analysis. Let us mention, for instance, silo processing where opening and closing of the bin gate induces complex stress redistribution, oedometer test for soils, casting modelling, where reverse deformation is of primary importance since it may lead to distortion of the required model shape.

2. Constitutive equations

Consider an isothermal deformation process of an initially isotropic and homogenous material. Assume small strain theory and neglect viscosity effects. If the actual stress state satisfies the yield condition, any stress increment $d\sigma_{ij}$ directed to the exterior of the yield surface induces the strain increment $d\varepsilon_{ij}$ which can be decomposed into two parts $d\varepsilon'_{ij}$ and $d\varepsilon''_{ij}$, thus

$$d\varepsilon_{ij} = d\varepsilon'_{ij} + d\varepsilon''_{ij}, \tag{2.1}$$

where $d\varepsilon'_{ij}$ and $d\varepsilon''_{ij}$ are for generality identified as hypoelastic and plastic increments, respectively. For the stress increment directed to the interior of the yield surface, only hypoelastic term $d\varepsilon'_{ij}$ occurs. Assume that stress has been applied to the material element which possesses the density ϱ_0. During the deformation process the density ϱ varies, and the increments satisfy the relations

$$d\varrho = \varrho_0 d\varepsilon_{ii}, \quad d\varrho' = \varrho_0 d\varepsilon'_{ii}, \; d\varrho'' = \varrho_0 d\varepsilon''_{ii}, \quad d\varrho = d\varrho' + d\varrho'', \tag{2.2}$$

where $d\varrho'$ and $d\varrho''$ denote reversible and irreversible density increments.

The constitutive equations are assumed in the form (see [12, 13, 14, 15, 18])

$$d\varepsilon_{ij} = \begin{cases} A_{ijkl} d\sigma_{kl} + \dfrac{1}{H} \dfrac{\partial f}{\partial \sigma_{ij}} df, & \text{for} \quad f = 0, \; df = 0, \\ A_{ijkl} d\sigma_{kl}, & \text{for} \quad f < 0, \quad \text{or} \quad f = 0, \; df < 0, \end{cases} \tag{2.3}$$

where $df_\sigma = (\partial f / \partial \sigma_{kl}) d\sigma_{kl}$ and A_{ijkl} denotes the matrix of hypoelastic compliance; H denotes the hardening or softening modulus and is proportional to tangent modulus in the uniaxial case. Assuming the yield condition in the form

$$f(\sigma_{ij}, \varrho'') = 0, \tag{2.4}$$

the hardening modulus is expressed as follows:

$$H = \frac{\partial f}{\partial \sigma_{ii}} \varrho_0 \left(- \frac{\partial f}{\partial \varrho''} \right). \tag{2.5}$$

Let un note that compressive stresses and strains are assumed as positive. Since $\partial f / \partial \varrho'' < 0$, the hardening parameter is positive for those stress states for which $f_{,ii} \equiv \equiv \partial f / \partial \sigma_{ii} > 0$; when $f_{,ii} < 0$ the softening occurs and the yield surface shrinks during the deformation.

In order to construct a simple constitutive relation, let us assume that material function tensor A_{ijkl} is isotropic and depends only on density change portions ϱ', ϱ'' and on ϱ_0 but not on the strain or stress tensors. Note that the form of the yield condition (2.4) also follows from the neglect of anisotropic hardening effects and the same may be said about the plastic hardening moduli tensor $\frac{1}{H} \partial f / \partial \sigma_{ij} \; \partial f / \partial \sigma_{kl}$ in the Eq. (2.3).

Thus in the deformed state, the incremental behaviour is purely isotropic, since no preferred orientation is induced by previous prestrain. Thus, we can write

$$d\sigma_{kk} = K(\varrho', \varrho'', \varrho_0) d\varepsilon'_{kk}, \quad ds_{kl} = G(\varrho', \varrho'', \varrho_0) de'_{kl}, \tag{2.6}$$

where de'_{kl} and ds_{kl} denote deviatoric parts of strain and stress increment tensors; K and G stand for volumetric and shear incremental stiffness moduli. Relations (2.6) imply coaxiality of stress and strain increment tensors.

When unloading occurs from some state on the yield surface, both ϱ_φ and ϱ'' are fixed, and then K and G depend only on reversible density variation. On the other hand, for loading process involving plastic strains, the density parts ϱ' and ϱ'' vary and stiffness moduli change their values with both reversible and irreversible density changes. The initial density ϱ_0 is fixed for a single test, but may vary from test to test due to different preconsolidation.

To clarify the material behaviour in the hypoelastic domain, consider a closed stress cycle OABCO, shown in Fig. 1a. It consists of shear within the yield surface with super-

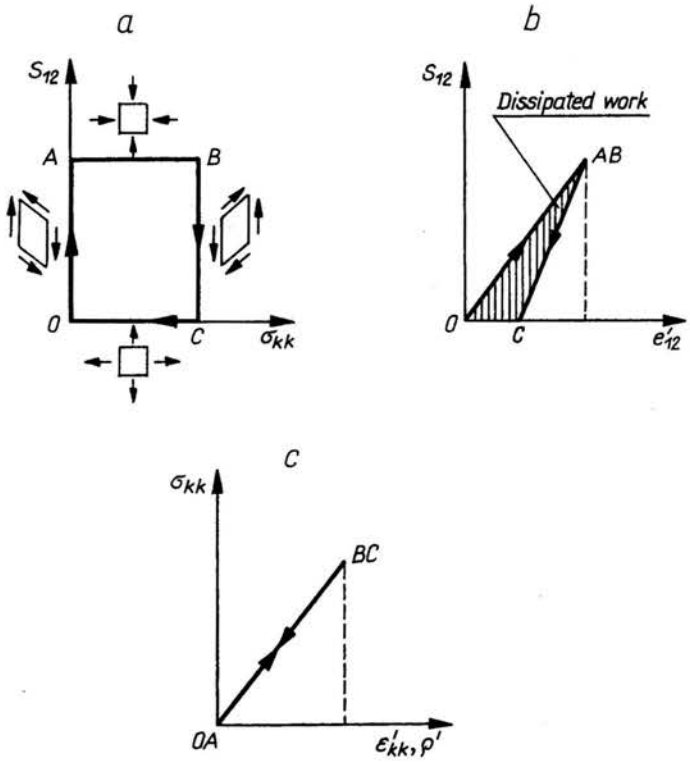

FIG. 1. a. Closed stress cycle. b. Shear response. c. Volumetric response.

posed hydrostatic compression which consolidates the material; the cycle is completed by removing shear stress and next hydrostatic pressure. Since along AB the density ϱ' increases, the modulus G increases and unloading along BC occurs for greater value of ϱ' than at the point A. Thus a permanent shear strain remains after completing the cycle and the work expended during this cycle does not vanish: it is equal to the dashed area shown in Fig. 1b. By reversing the cycle, this work becomes negative. Since this prediction is not realistic, the applicability of model of hypoelastic material is limited to nearly radial loading or deformation paths and to single unloading. For multi-cyclic loading, the purely elastic behaviour should be expected within the yield surface, and the strain or stress energy functions should be used in deriving constitutive relations. Application of the term "hypoelasticity" referring to the Eqs. (2.6) is convenient here and is fully legitimate since,

due to integrability of (2.6), moduli K and G may be expressed as functions of the mean pressure σ_{kk} for fixed ϱ_0.

Let us now consider specific forms of (2.6). Assume that the initial density ϱ_0 is fixed. To investigate coupling effects between reversible and irreversible density changes, let us assume two extreme cases: first, we postulate that $K = K(\varrho_0, \varrho')$, $G = G(\varrho_0, \varrho')$ and irreversible part of density ϱ'' does not affect the stiffness moduli; second, we assume that $K = K(\varrho_0, \varrho)$, $G = G(\varrho_0, \varrho)$, that is the total density $\varrho = \varrho' + \varrho''$ defines the material functions. Using polynomial representation for the first assumption we can write

$$K = K_0\Big[1 + \sum_1^m \alpha_s(\bar{\varrho}' - 1)^s\Big], \quad G = G_0\Big[1 + \sum_1^n \beta_s(\bar{\varrho}' - 1)^s\Big], \tag{2.7}$$

where K_0, G_0, α_s and β_s are functions of initial density and $\bar{\varrho}' = \varrho'/\varrho_0$. For the second model we have correspondingly

$$K = K_0\Big[1 + \sum_1^m \alpha_s(\bar{\varrho} - 1)^s\Big], \quad G = G_0\Big[1 + \sum_1^n \beta_s(\bar{\varrho} - 1)^s\Big], \tag{2.8}$$

where $\bar{\varrho} = \varrho/\varrho_0$.

These two types of relationships can easily be visualized by using the diagram σ_{kk} versus ε_{kk}, shown in Fig. 2. The portion OA represents the elastic behaviour before the first

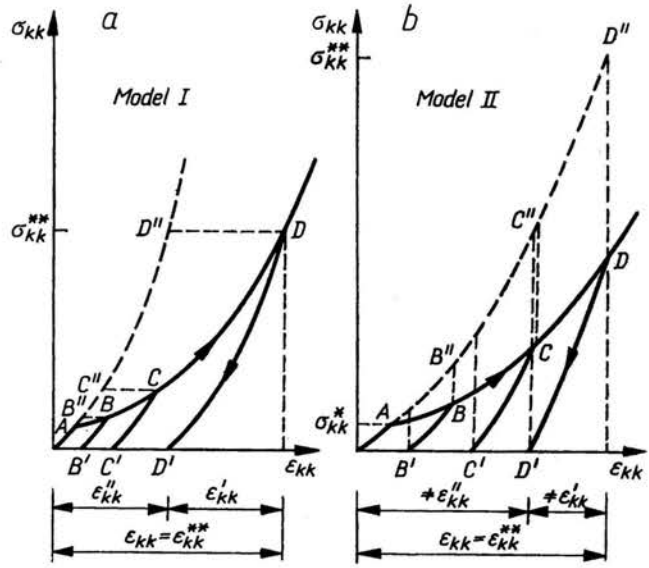

FIG. 2. Loading and unloading behaviour of model I and model II for purely hydrostatic stress state.

yield, whereas the portion AD corresponds to elastic-plastic behaviour. Consider now unloading curves from points B, C, D. If the model (2.7) applies, the curves BB', CC' and DD' would be identical to the portions OB'', OC'' and OD'' of the elastic compression curve OD''. Thus any unloading curve is obtained by translation of OD'' along the ε_{kk} axis to the respective point on AD. On the other hand, if the hypothesis (2.8) is assumed,

the unloading curves BB', CC' and DD' are obtained by translation of the elastic compression curve along the σ_{kk} axis; in fact, now these curves depend on total density change rather than reversible part of ϱ. This geometrical property facilitates experimental check of postulated relations. It is obvious that there is a significant difference in unloading behaviour depending on the type of assumed relationship (2.7) or (2.8).

Consider now the plastic behaviour for increasing stress. Assume the yield condition in the form

$$f_q = (I_2')^{\frac{1}{2}} \pm a_q I_1 - \varkappa_q = 0, \tag{2.9}$$

where

$$I_1 = \sigma_{kk},\ I_2 = \frac{1}{2} s_{ij} s_{ij}, \quad a_q = \text{const},\ \varkappa_q = \varkappa_q(\bar{\varrho}''), \quad q = 1, 2.$$

This yield condition is represented in the space of principal stresses by two coaxial cones $f_1 = 0$ and $f_2 = 0$, Fig. 3a, and thus assures plastic yield even for purely hydrostatic stress state. Using polynomial representation for the functions $\varkappa_q(\bar{\varrho}'')$ we have

$$\varkappa_1 = \varkappa_{10}\left[1 + \sum_1^u \gamma_s (\bar{\varrho}'')^s\right] \tag{2.10}$$

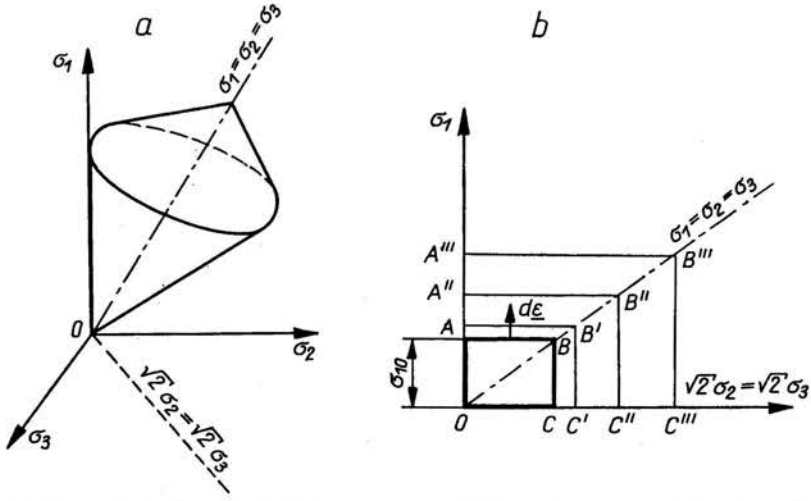

FIG. 3. a. Yield surface in the principal stress space. b. Yield surface representation for axi-symmetric stress state.

and similar relation for $\varkappa_2$. If we restrict our consideration to hardening domain, only the conical surface $f_1 = 0$ is of interest. Using (2.5), the hardening modulus is now expressed as follows

$$H = a_1 \varkappa_{10} \varrho_0 \sigma_{kk} \sum_1^u [s\gamma_s (\bar{\varrho}'')^{s-1}]. \tag{2.11}$$

3. Uniaxial strain problem

In order to compare the behaviour of models presented with that of real material, the tests were carried out on several granular media. The simple uniaxial strain state test was chosen for which the theoretical solution is presented below.

For the uniaxial strain problem, the stress and strain states are described by the following relations, Fig. 4,

$$\varepsilon_1 > 0, \quad \varepsilon_2 = \varepsilon_3 = 0, \quad \sigma_1 > 0, \quad \sigma_2 = \sigma_3 > 0,$$

$$\varepsilon_{kk} = \varepsilon_1, \quad e_1 = -2e_2 = \frac{2}{3}\varepsilon_1, \tag{3.1}$$

$$\sigma_{kk} = \sigma_1 + 2\sigma_2, \quad s_1 = -2s_2 = -2s_3 = \frac{2}{3}(\sigma_1 - \sigma_2).$$

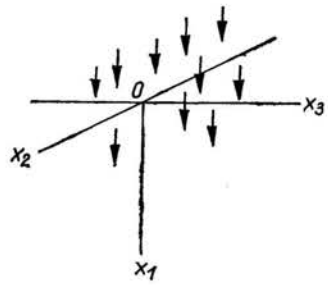

FIG. 4. Uniaxial strain problem.

For numerical calculation we assume that both softening and hardening cones of the yield surface posess the apex angle equal to $\pi/2$. Hence the yield condition (2.9) reduces to the form, Fig. 3/b,

$$\sigma_1 = \sigma_{10}\Big[1 + \sum_1^u \gamma_s(\bar{\varrho}'')^s\Big], \quad \text{or} \quad \sigma_2 = 0, \quad \text{for} \quad \sigma_1 > \sigma_2, \tag{3.2}$$

where σ_{10} denotes the stress when the first yield occurs. Due to the relations (3.1) both isotropic and deviatoric parts of the strain-increment tensor in (2.6) become functions of the axial strain only. In this case, the Eq. (2.6) is integrable and results in non-linear elastic-plastic constitutive relations.

i) Elastic solution: loading. In the elastic state, when $f < 0$, we have $\varrho'' = 0$, $\varrho' = \varrho$, and both proposed models coincide. After substituting the relations (2.8) into (2.3), the following relation between stress-increments can be written

$$d\sigma_2 = \frac{K(\varrho) - G(\varrho)}{2G(\varrho) + K(\varrho)}\, d\sigma_1. \tag{3.3}$$

On integrating the Eqs. (2.6) and making use of the Eqs. (2.2), (2.7), (3.3) with the initial condition $\bar{\varrho} = 1$ for the stress-free state, we have:

$$\sigma_1 = \frac{G_0}{3}\left[h_0(\bar{\varrho} - 1) + \sum_1^P \frac{1}{s+1} h_s(\bar{\varrho} - 1)^{s+1}\right],$$

$$\sigma_2 = \frac{G_0}{3}\left[l_0(\bar{\varrho} - 1) + \sum_1^P \frac{1}{s+1} l_s(\bar{\varrho} - 1)^{s+1}\right], \tag{3.4}$$

where

$$h_0 = \frac{K_0}{G_0}+2, \quad h_s = 2\beta_s+\frac{K_0}{G_0}\alpha_s,$$

$$l_0 = \frac{K_0}{G_0}-1, \quad l_s = -\beta_s+\frac{K_0}{G_0}\alpha_s,$$

and p is equal to the greater value from among m and n appearing in the Eqs. (2.7) and (2.8). The strain ε_1 is related to the density by the equation $\varepsilon_1 = \bar{\varrho}-1$. The solution given by the Eqs. (3.4) holds before the first yield occurs. Substituting $\sigma_1 = \sigma_{10}$ into the Eq. $(3.4)_1$ one can find the strain ε_1^* and the density $\bar{\varrho}^*$, and then using the Eq. $(3.4)_2$ — the stress tensor σ_{kl}^* corresponding to the initial yield.

ii) Elastic-plastic solution: loading. If we suppose that both plastic and elastic consolidation is provided simultaneously ($\varepsilon'_{kk} > 0$, $\varepsilon''_{kk} > 0$), the only admissible stress states are represented in Fig. 3b by the points on the sides AB, $A'B'$ ... corresponding to the hardening domain of the yield condition. Since $d\varepsilon''_2 = 0$ for AB, $A'B'$ ... and $\varepsilon_2 = 0$ in view of the Eq. (2.1), there is $d\varepsilon'_2 = 0$. Therefore, the relations (3.3) hold true for the plastic state, having the new parameter $\varrho = \varrho' + \varrho''$. Making use of the Eqs. (3.3) and $(2.6)_1$, the elastic density increment can now be expressed in the form

$$d\varrho' = \frac{3}{2G(\bar{\varrho})+K(\bar{\varrho})}\,d\sigma_1. \tag{3.5}$$

To determine the plastic density-increment the yield condition (3.2) has to be differentiated, and

$$d\bar{\varrho}'' = \frac{d\sigma_1}{\sigma_{10}\sum_1^u s\gamma_s(\bar{\varrho}'')^{s-1}}. \tag{3.6}$$

The set of the non-linear ordinary differential equations (3.5), (3.6) has different forms for the two models (2.7) and (2.8). The initial conditions are given by σ_{kl}^*, $\bar{\varrho}^*$ which are known from the elastic solution.

For the model I, the Eqs. (3.5) and (3.6) result in the following set of algebraic equations

$$\sigma_{kk} = K_0\left[(\bar{\varrho}'-1)+\sum_1^m \frac{1}{s+1}\alpha_s(\bar{\varrho}'-1)^{s+1}\right]+\sigma_{kk}^*,$$

$$\sum_1^u \gamma_s(\bar{\varrho}'')^s = \frac{G_0}{3\sigma_{10}}\left[h_0(\bar{\varrho}'-1)+\sum_1^p \frac{1}{s+1}h_s(\bar{\varrho}'-1)^{s+1}\right]-1, \tag{3.7}$$

$$\sigma_1 = \sigma_{10}\left[1+\sum_1^u \gamma_s(\bar{\varrho}'')^s\right], \quad \sigma_2 = \frac{\sigma_{kk}-\sigma_1}{2},$$

where h_0, h_s and p are defined in (3.4). For given $\bar{\varrho}'$, one can find from the Eqs. (3.7) the value of ϱ'', and the corresponding stresses. The analytical solution exists for the linear hardening rule (2.10).

For the model II, the closed-form solution of the Eqs. (3.5), (3.6) cannot be found in general case except for the linear hardening rule (2.10). The solution can be obtained by carrying out step by step numerical integration, replacing differentials by small increments. Assuming an increment of $\Delta\sigma_1$ one can find the associated $\Delta\bar{\varrho}'$ and $\Delta\bar{\varrho}''$, and afterwards $\Delta\bar{\varrho}$ and $\Delta\sigma_2$. Summation of subsequent increments gives the current values of $\bar{\varrho}$, σ_1 and σ_2.

iii) Elastic solution: unloading. To consider unloading from a plastic state it is supposed that loading stops at a stress level $\sigma_1 = \sigma_1^{**}$, $\sigma_2 = \sigma_2^{**}$ and at the corresponding densities $\bar{\varrho}' = \bar{\varrho}'^{**}$, $\bar{\varrho}'' = \bar{\varrho}''^{**}$. The behaviour of the material during unloading is described by the Eqs. (2.6). For the model I, the stress-strain relations for unloading are identical with (3.4). This is due to existence of the one-to-one relation between σ_{kl} and ε'_1 for both elastic and plastic loading process. Replacing in the Eqs. (3.4) the density $\bar{\varrho}$ by $\bar{\varrho}' = \bar{\varrho} - \bar{\varrho}''^{**}$ and writing densities in terms of strains, we have the total stress-strain relation. For the model II, the moduli K and G during unloading depend on the total density $\bar{\varrho}$. Therefore, the Eqs. (2.6) are not integrable with respect to $\bar{\varrho}'$ and the stress-strain relation is not directly available. However, for unloading we have $d\bar{\varrho}' = d\bar{\varrho}$, since $\bar{\varrho}'' = \text{const}$ and the Eqs. (2.6) can be integrated with respect to $\bar{\varrho}$. The initial conditions are known from the preceding loading state. The resultant expressions for stresses are

$$\sigma_1 = \sigma_1^{**} + \frac{G_0}{3}\left\{h_0[(\bar{\varrho}-1)-(\bar{\varrho}^{**}-1)] + \sum_1^P \frac{1}{s+1} h_s[(\bar{\varrho}-1)^{s+1} - (\bar{\varrho}^{**}-1)^{s+1}]\right\},$$

(3.8)

$$\sigma_2 = \sigma_2^{**} + \frac{G_0}{3}\left\{l_0[(\bar{\varrho}-1)-(\bar{\varrho}^{**}-1)] + \sum_1^P \frac{1}{s+1} l_s[(\bar{\varrho}-1)^{s+1} - (\bar{\varrho}^{**}-1)^{s+1}]\right\},$$

where h_0, l_0, h, l_s and p are determined by (3.4). The above solution holds true for unloading so long as the stress state is within the yield condition. In the case of reverse yielding on OA, Fig. 3b, the problem may be considered in a manner similar to that discussed in ii).

It is worth noting that when no reverse yield occurs the reloading and unloading processes are identical.

4. Experiments

In the experiments the agricultural granular materials: wheat grains and rice grains were used. For comparison, medium sand and rubber spheroids were also tested. The uniaxial strain state was obtained in a simple device, schematically presented in Fig. 5. The material filling the device was loaded and unloaded with constant velocity of displacement of the upper plate, $v = 0.2$ mm/min. To diminish the wall friction, the inner surface of the device was greased. The vertical and radial stresses σ_1 and σ_2 were measured by means of strain-gauge transducers, mounted at the gaps of the thickwalled ring and on the upper plate. The transducers were designed to ensure the radial displacement of the ring to be negligibly small.

In Fig. 6 the measured mean dependence of σ_1 on ε_1 for materials tested is plotted; qualitatively similar behaviour and non-linearity during loading and unloading are observed. The elaboration of these results in view of the models proposed may be made directly by appropriate comparison of subsequent unloading curves following the shifting rules described in Sec. 3 (see Fig. 2). Besides inquiring which of the models fits better to the results obtained, the tests were aimed at determination of material functions appearing in the Eqs. (2.3). The material functions were evaluated along the procedure described in Appendix. Below the results for wheat grains are presented.

Figure 7 presents the measured relationships σ_1 versus ε_1 and σ_2 versus ε_1, from which curves were found for σ_{kk} versus ε_{kk} and s_1 versus e_1. These curves were next approximated

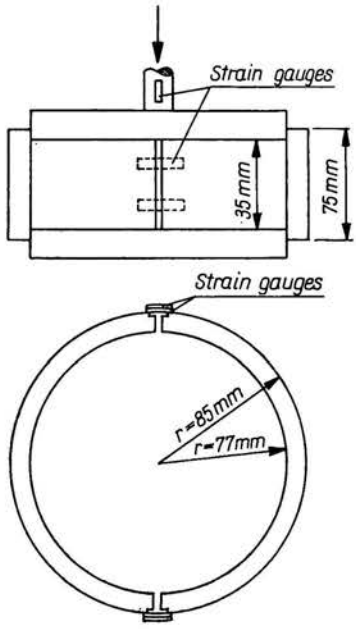

FIG. 5. Scheme of uniaxial strain device.

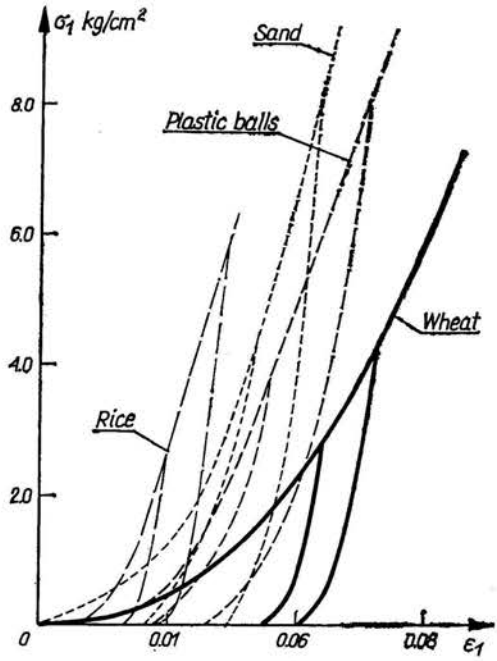

FIG. 6. Experimental curves σ_1 *vs.* ε_1 for tested materials.

following the appropriate procedure for model I and II. The same simple form of polynomials for moduli K and G and both models was assumed, thus providing the information on the coupling effect. For the same reason, the yield condition and the hardening rule were chosen in the same form for both models. The following numerical values for material constants were obtained:

for model I

$$K = K(\bar{\varrho}') = K_0[1+\alpha_2(\bar{\varrho}'-1)^2], \quad G = G(\bar{\varrho}') = G_0[1+\beta_1(\bar{\varrho}'-1)],$$

where

$$K_0 = 10 \text{ kg/cm}^2, \qquad \alpha_2 = 156\,000,$$
$$G_0 = 14.025 \text{ kg/cm}^2, \qquad \beta_1 = 618,$$

for model II

$$K = K(\bar{\varrho}) = K_0[1+\alpha_2(\bar{\varrho}-1)^2], \quad G = G(\bar{\varrho}) = G_0[1+\beta_1(\bar{\varrho}-1)],$$

where

$$K_0 = 47.62 \text{ kg/cm}^2, \qquad \alpha_2 = 4200,$$
$$G_0 = 9.52 \text{ kg/cm}^2, \qquad \beta_1 = 105,$$

and

$$\sigma_1 = \sigma_{10}[1+\gamma_1\bar{\varrho}''+\gamma_3(\bar{\varrho}'')^3],$$

where

$$\sigma_{10} = 0.005 \text{ kg/cm}^2, \quad \gamma_1 = 100, \quad \gamma_3 = 1\,290\,000.$$

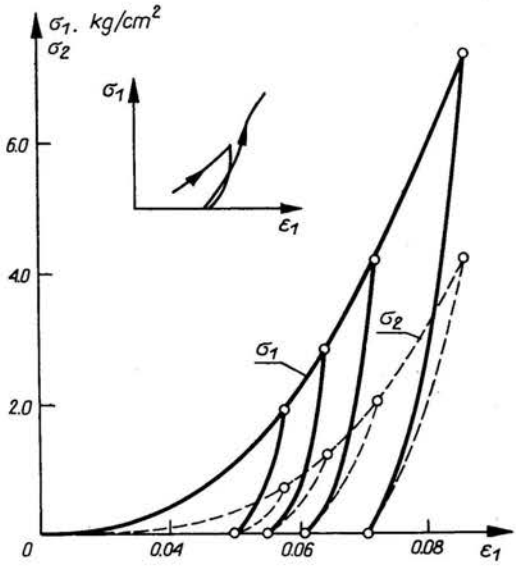

FIG. 7. Experimental curves σ_1 *vs.* ε_1 and σ_2 *vs.* ε_2 for wheat grains.

Figures 8 and 9 present the comparison of the experimental and theoretical relationships σ_1 versus ε_1. For model II, the theoretical curves were found by numerical integration of the Eqs. (3.5) and (3.6) with varying step of $\Delta\sigma_1$ ranging from 0.1 to 0.5 kg/cm². Inspection of Figs. 8 and 9 indicates that model I gives better agreement for unloading process, though discrepancy exists. Regarding relationships σ_1 versus σ_2, Figs 10a and 10b, both models lead to discrepancy with experiments. For model II, however, the loading and unloading paths are described differently, what is in agreement with experiments. For model I, because of (3.5), the paths coincide.

The above analysis may indicate that in the material investigated the coupling of reversible and irreversible deformations really exists, though is not so strong as it was assumed in the model II. The other forms of the Eqs. (2.6) may easily be investigated within the theory.

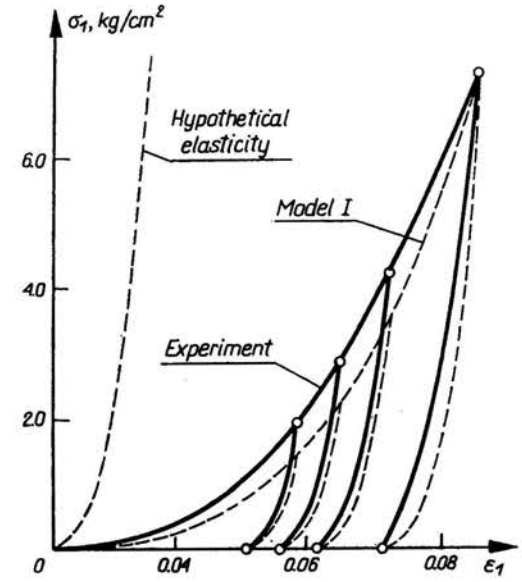

FIG. 8. Wheat grains. Experimental and theoretical curves for uniaxial test. Model I.

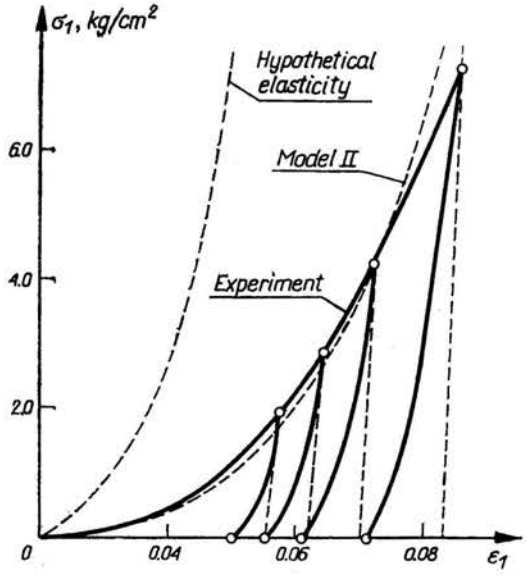

FIG. 9. Wheat grains. Experimental and theoretical curves for uniaxial test. Model II.

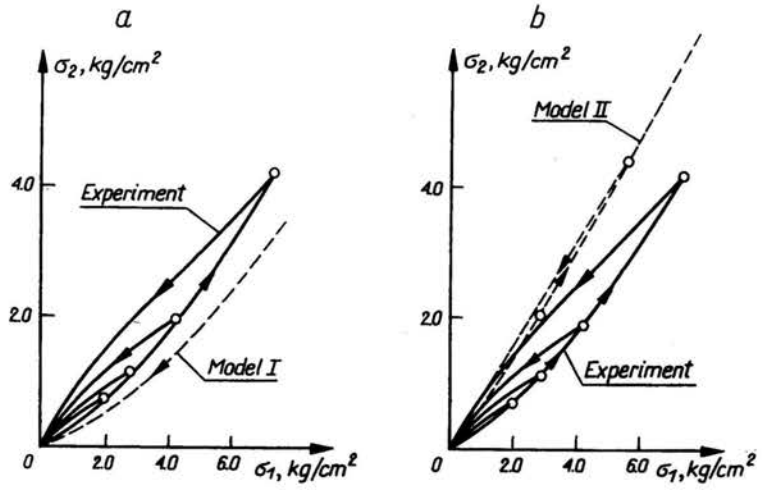

FIG. 10. Wheat grains. Experimental and theoretical curves for uniaxial test. σ_2 *vs.* σ_1 response.

5. Concluding remarks

The simple tests discussed in this paper provided sufficient data in order to determine both hardening modulus and hypoelastic functions and relate them to variable density. Although not very significant, the coupling effect between reversible and irreversible density changes is present and may be more important in the range of lower densities. On the other hand, the assumption that total density defines the hypoelastic moduli was proved to be incorrect. Thus describing plastic and hypoelastic or elastic behaviour it is necessary to decompose total volume or density changes into reversible and irreversible parts.

Acknowledgement

The authors are deeply indebted to Professor Z. MRÓZ for his inspiration and helpful discussion of this paper.

Appendix

The procedure of determining the material functions presented below is referred to uniaxial strain state only. In this state the behaviour is elastic-plastic, and the shifting rules from Fig. 2 hold for both volumetric and deviatoric relationships.

Elasticity. In order to evaluate the elastic constants appearing in the Eqs. (2.6), the experimental results either for loading (before the first yield occurs) or for unloading can equivalently be used. However, there is no difference between the models before initial yielding, and thus for choice of model the unloading curves have to be taken.

Model I. Due to the lack of coupling between elastic and plastic properties the experimental curves for unloading process directly define the relationships σ_1 versus ε_1' and σ_2 versus ε_1', (see Fig. 2). From these relationships the curves σ_{kk} versus ε_{kk}' and s_1 versus e_1' can be constructed, and then the curves $d\sigma_{kk}/d\varepsilon_{kk}'$ versus $\bar{\varrho}'-1$ and ds_1/de_1' versus $\bar{\varrho}'-1$ can be found, Fig. 11a. For model I, the subsequent curves should coincide (horizontal shifting principle). The coefficients of polynomials approximating the curves define the constants K_0, G_0, α_s and β_s. If moduli K_0 and G_0 are supposed to be greater than zero,

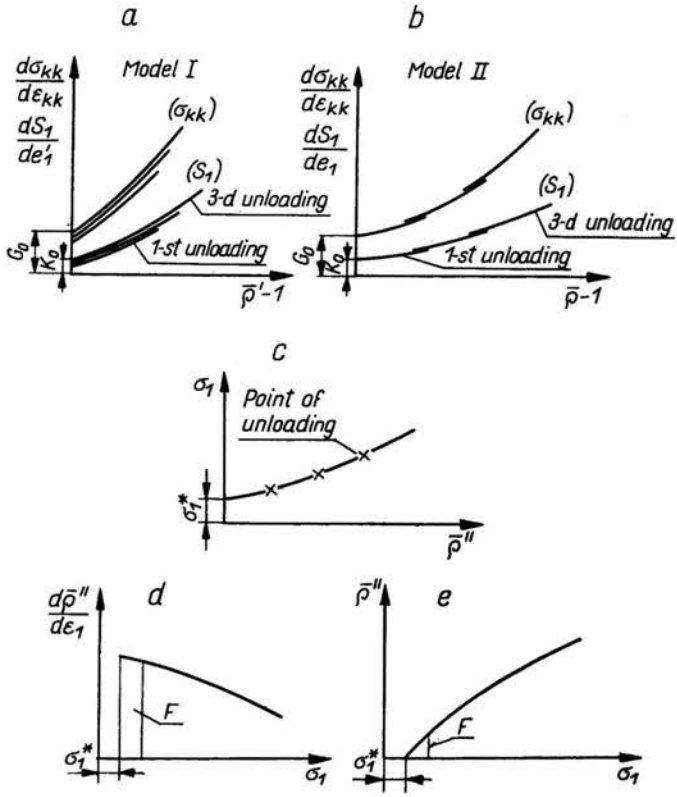

FIG. 11. Schematic plots for determination of material functions.

the polynomials must contain a free term. To check the magnitude of K_0 and G_0 moduli, the following relation resulting from the Eqs. (2.7) and (3.3) for $\bar{\varrho}'-1=0$ can be used

$$\frac{G_0}{K_0} = \frac{1-(d\sigma_2/d\sigma_1)_{\sigma_1=0}}{2[(d\sigma_2/d\sigma_1)_{\sigma_1=0}+1]}, \tag{A.1}$$

where the ratio $(d\sigma_2/d\sigma_1)_{\sigma_1=0}$ is known from the experiments. The elastic constants may also be found by direct approximation of σ_{kk} versus ε_{kk}' and s_1 versus e_1' curves by polynomials and then, after differentiation, by identification with the coefficients in (2.7).

Model II. The coupling existing in the model II does not allow for the determination of elastic and plastic strain directly from the unloading curves (see Fig. 2.). We note, however, that the slope of any unloading curve determines the ratio of stress-increment to

the elastic strain-increment. Thus, from the relationships σ_{kk} versus ε_{kk} and s_1 versus e_1 for unloading, the slopes $d\sigma_{kk}/d\varepsilon'_k$ and ds_1/de'_1 for given total density can be found. According to the principle of vertical shifting, the curves $d\sigma_{kk}/d\varepsilon'_{kk}$ versus $\bar{\varrho}-1$ and ds_1/de'_1 versus $\bar{\varrho}-1$ should respectively coincide, Fig. 11b. The coefficients of polynomials approximating the last curves determine the elastic parameters. It is also possible to construct first the hypoelastical elastic curve, and then to differentiate the approximating polynomial. The initial moduli are still defined by the Eq. (A.1).

Plasticity. For the assumed yield condition the initial yield stress σ_1^* is for both models equal to the maximum values of stress on σ_1 versus ε_1 plot for which the loading and unloading curves still coincide. The determination of hardening rule for both models has to be made in a different way.

Model I. Having known for the loading curve σ_1 versus ε_1 the values of density ϱ'' for unloading points, we can construct the curve σ_1 versus $\bar{\varrho}''$, Fig. 11c. Now, the approximation by polynomial can be made.

Model II. For the determination of coefficients γ_s it is necessary, like in model I, to construct the curve σ_1 versus $\bar{\varrho}''$. The evaluation of $\bar{\varrho}''$ has to be done as follows. Instead of $d\sigma_1/d\bar{\varrho}''$, in view of (2.2), we can write

$$\frac{d\bar{\varrho}_1}{d\varrho''} = \frac{d\sigma_1}{d\bar{\varrho}} \frac{d\bar{\varrho}}{d\bar{\varrho}''} = \frac{d\sigma_1}{d\bar{\varrho}} \left(\frac{d\bar{\varrho}'}{d\bar{\varrho}''} + 1 \right). \tag{A.2}$$

The value of $d\bar{\varrho}'/d\bar{\varrho}''$ may be found by substituting (3.5) into (3.6). Thus the Eq. (A.2) can be expressed in the form:

$$\frac{d\sigma_1}{d\bar{\varrho}''} = \frac{d\sigma_1/d\bar{\varrho}}{1-3(d\sigma_1/d\bar{\varrho})\{2G(\bar{\varrho})+K(\bar{\varrho})\}^{-1}}. \tag{A.3}$$

Here $d\sigma_1/d\bar{\varrho}$ is the value of derivative of the experimental curve σ_1 versus $\bar{\varrho}$. K and G are known from the elastic solution. For a given σ_1 and corresponding $\bar{\varrho}$ one can find from the Eq. (A.3) the value of $d\sigma_1/d\bar{\varrho}''$ and hence $d\bar{\varrho}''/d\sigma_1$. It is convenient to plot the function $d\bar{\varrho}''/d\sigma_1$ versus σ_1, Fig. 11d, and after graphical integration to find the relation $\bar{\varrho}''$ versus σ_1, Fig. 11e. The inversion of the last plot and the approximation by the polynomial determines the hardening rule and its parameters γ_s.

References

1. I. HOLUBEC, *Elastic behaviour of cohesionless soil*, Proc. Am. Soc. Civ. Engrs, **94**, SM 6, 1215–1231, 1968.
2. H. Y. KO and R.F. SCOTT, *Deformation of sand in hydrostatic compression*, Proc. Am. Soc. civ. Engrs, **93**, SM 3, 137–156, 1967.
3. H. Y. KO and R. F. SCOTT, *Deformation of sand in shear*, Proc. Am. Soc. civ. Engrs, **93**, SM 5, 283–310, 1967.
4. D. C. DRUCKER, R. E. GIBSON and D. J. HENKEL, *Soil mechanics and work-hardening theories of plasticity*, Trans. Am. Soc. civ. Engrs, **122**, 338–346, 1957.
5. A. W. JENIKE and R. T. SHIELD, *On the plastic flow of Coulomb solids beyond original failure*, J. Appl. Mechs, **26**, 599–602, 1959.
6. K. H. ROSCOE and H. B. POOROOSHASB, *A theoretical and experimental study of strains in triaxial tests on normally consolidated clays*, Geotechnique, **13**, 12–38, 1963.

7. K. H. ROSCOE and J. BURLAND, in Engineering Plasticity, ed. J. HEYMAN and F. A. LECKIE, Cambrigde Univ. Press, 1968.
8. J. B. WEIDLER and P. R. PASLAY, *Constitutive relations for inelastic granular medium*, Proc. Am. Soc. civ. Engrs, **96**, EM 4, 395–406, 1970.
9. P. WROTH and A. SCHOFIELD, *Critical state soil mechanics*, McGraw Hill, London 1968.
10. V. N. NIKOLAIEVSKII, *Constitutive equations for plastic deformations of granular media* [in Russian], Prikl. Mat. Mekh., **35**, 1070–1082, 1971.
11. A. SAWCZUK and P. STUTZ, *Contribution à l'étude de loi constitutive des milieux pulvérulents*, Problèmes de la Rhéologie, ed. W. K. NOWACKI, 319–334, PWN, Warsaw 1973.
12. Z. MRÓZ and A. DRESCHER, *Limit plasticity approach to some cases of flow of bulk solids*, J. Enging for Industry, **91**, 357–364, 1969.
13. A. DRESCHER, *Experimental verification of body with density hardening* [in Polish], Rozpr. Inżyn. **20**, 351–387, 1972.
14. Z. MRÓZ and K. KWASZCZYNSKA, *Some boundary-value problems for density-hardening media* [in Polish], Rozpr. Inżyn. **19**. 15–42, 1971.
15. T. HUECKEL and Z. MRÓZ, *Some boundary-value problems for variable density materials*, Proc. Problèmes de la Rhéologie, ed. W. K. NOWACKI, 173–191, PWN, Warsaw 1973.
16. M. D. COON and R. J. EVANS, *Recoverable deformation of cohesionless soils*, Proc. Am. Soc. Civ. Engrs, **97**, SM 2, 375–391, 1971.
17. I. NELSON and M. L. BARON, *Application of variable moduli models to soil behavior*, Int. J. Solids Struct. **7**, 399–418, 1971.
18. T. HUECKEL, *A note on the behaviour of hardening-softening granular media*, Problèms of Plasticity. ed. A. SAWCZUK, 397–402, Noordhoff Int. Publ., 1974.
19. G. Y. BALADI, *The latest development in the non-linear elastic-nonideally plastic work-hardening cap model*, Proc. Symp. Role of Plasticity in Soil Mechanics, Cambridge, 51–55, 1973 [discussion].

POLISH ACADEMY OF SCIENCES
INSTITUTE OF FUNDAMENTAL TECHNOLOGICAL RESEARCH.

Received March 27, 1974.